

## Supplementary Materials for

### **Electric-field control of spin dynamics during magnetic phase transitions**

Tianxiang Nan\*, Yeonbae Lee, Shihao Zhuang, Zhongqiang Hu, James D. Clarkson, Xinjun Wang, Changhyun Ko, HwanSung Choe, Zuhuang Chen, David Budil, Junqiao Wu, Sayeef Salahuddin, Jiamian Hu, Ramamoorthy Ramesh\*, Nian Sun\*

\*Corresponding author. Email: [nantianxiang@mail.tsinghua.edu.cn](mailto:nantianxiang@mail.tsinghua.edu.cn) (T.N.); [rramesh@berkeley.edu](mailto:rramesh@berkeley.edu) (R.R.); [n.sun@northeastern.edu](mailto:n.sun@northeastern.edu) (N.S.)

Published 2 October 2020, *Sci. Adv.* **6**, eabd2613 (2020)  
DOI: 10.1126/sciadv.abd2613

#### **This PDF file includes:**

Figs. S1 to S3

## 1. Thin film structural characterization in FeRh/PMN-PT.

X-ray diffraction (XRD) experiments were performed using the Panalytical X'Pert Pro diffractometer by Philips with Cu  $K\alpha_1$  radiation. **Figure S1** shows the  $2\theta$ - $\theta$  scan of a 50-nm-thick FeRh film grown on a (001)-oriented PMN-PT substrate. The FeRh films show typical characteristics of epitaxial growth and its crystal direction aligned with the orientation of PMN-PT substrate along the (001)-direction.

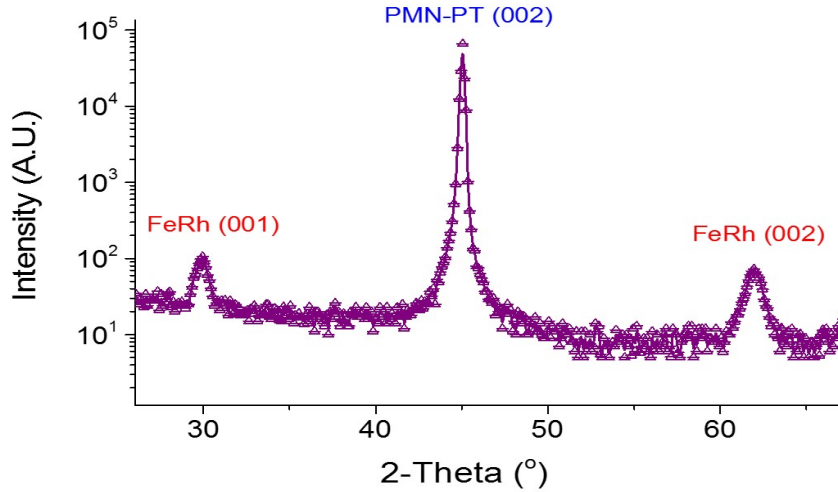


**Figure S1.** XRD spectrum of a FeRh/PMN-PT heterostructure grown by DC sputtering technique. Both the (001) and (002) peaks of FeRh are identified and aligned parallel to the (002) plane of the PMN-PT substrate.

## 2. Temperature and electric field dependence of electrical transport measurements.

Temperature  $T$  dependence of resistivity  $\rho$  measurement was carried out in a typical four-probe stage setup utilizing the van der Pauw geometry from the temperature  $T$  range of 300 to 420K. Both the external current source (Keithley-6220) and voltage meter (Keithley-2182) were used for resistivity measurement while DC electric fields  $E$ -field of up to  $\pm 0.67 \text{ V } \mu\text{m}^{-1}$  were provided by a Keithley-6517B voltage source, and applied between the top FeRh film and the bottom Au electrode. **Figure S4a** shows the plot of  $\rho$  vs.  $T$  at two different  $E$ -field states and clearly shows the shift in the magnetic phase transition temperature of up to 15 K between the value of  $E=0$  and  $E=+0.67 \text{ V } \mu\text{m}^{-1}$ . We also performed the  $E$  dependence of resistivity modulation, namely  $\Delta\rho$  vs.  $E$ , where  $\Delta\rho$  is defined by  $[\rho(E) - \rho_{\min}] / \rho_{\min}$  and  $\rho_{\min}$  is the minimum resistivity taken at a given isothermal  $\rho$ - $E$  curve on various temperatures as shown in the Figure S4a. In the plot of  $\Delta\rho$  vs.  $E$ , the temperature was various systematically and at a given temperature, resistivity was continuously measured by varying  $E$  in the range of  $-0.67$  and  $+0.67 \text{ V } \mu\text{m}^{-1}$ .

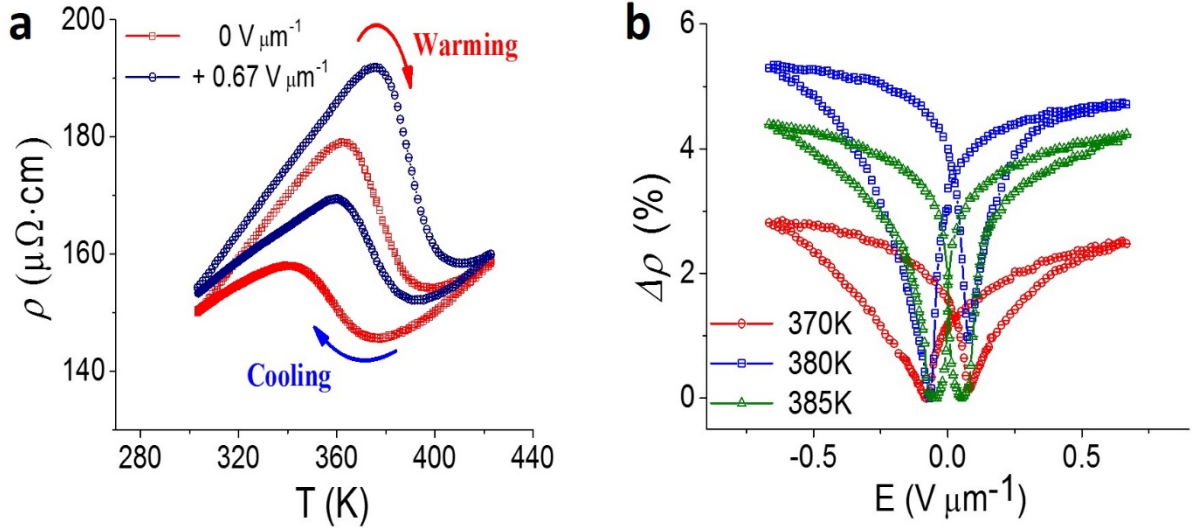


**Figure S2.** Electrical transport measurement of FeRh / PMN-PT heterostructure and modulation by external  $E$ . **(a)**  $\rho$ - $T$  curve for  $E$  values of 0 and  $+0.67 \text{ V } \mu\text{m}^{-1}$ . Hysteresis of the resistivity change is clearly visible, with the arrows indicating the warming (red) and cooling (blue) processes. **(b)** The isothermal plots of  $\Delta\rho$  versus  $E$  are plotted in  $T=370, 380,$  and  $385\text{K}$ . We noted that the  $\Delta\rho$ - $E$  curve show no noticeable change at  $T=420\text{K}$  (not shown in the figure), presumably due to strong ferrimagnet dominant state, and therefore shows little response to external strain modulation.

### 3. FMR absorption spectrum and the estimation of the ferromagnetic phase fraction.

In a well calibrated microwave cavity, the integral of FMR absorption spectrum over the field can be used to estimate the total resonant magnetic moment in the sample. During the phase transition in FeRh, although the ferromagnetic phase fraction changes drastically, the saturation magnetization in each ferromagnetic domain only changes slightly with temperature. We then estimate the ferromagnetic phase fraction by calculating the area under the FMR absorption curve as shown in Figure S3. The FMR absorption curve was obtained by the integral of FMR spectrum (Figure 1B) over the field.

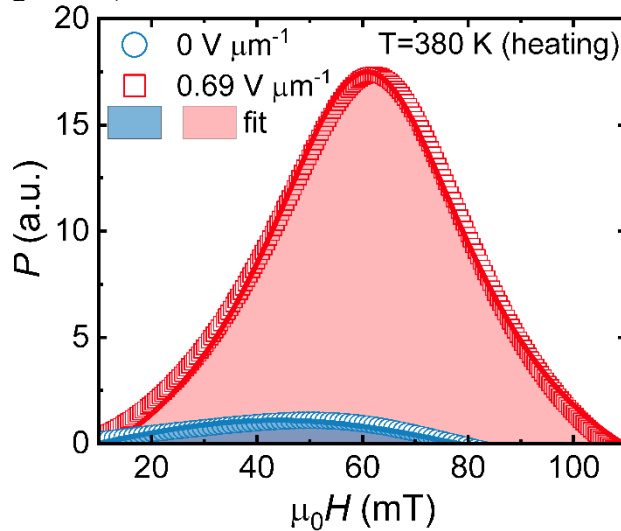


**Figure S3.** FMR absorption spectral for FeRh/PMN-PT at 380 K during heating with applied electric fields of  $0 \text{ V } \mu\text{m}^{-1}$  (blue) and  $0.67 \text{ V } \mu\text{m}^{-1}$  (red), respectively.